

**SPECTRAL CHARACTERIZATION AND MINERALOGY/CHEMISTRY OF OPALINE SILICA SAMPLES FROM DIVERSE MARS ANALOG SITES.** V. Z. Sun<sup>1</sup>, R. E. Milliken<sup>1</sup>, K. M. Robertson<sup>1</sup>, S. W. Ruff<sup>2</sup>, and J. D. Farmer<sup>2</sup>, <sup>1</sup>Dept. of Earth, Environmental, and Planetary Sciences, Brown Univ., RI 02912; <sup>2</sup>School of Earth and Space Exploration, Arizona State Univ., AZ 85287. (Vivian\_Sun@brown.edu)

**Introduction:** Opaline silica has been detected in a variety of locations on Mars [1], including *in situ* analysis at Gusev and Gale craters with the *Spirit* [2,3] and *Curiosity* [4,5] rovers, respectively. *Curiosity's* CheMin XRD instrument has identified significant amorphous components in several drill targets [6], some of which may represent opal-A. Other silica polymorphs such as cristobalite and tridymite have also been identified in these samples, leading to questions of their origins and implications for the ancient aqueous environment at Gale crater [4,5].

The formation of opaline silica requires interaction with water, but it is uncertain whether this environment was acidic [2,4,7,8] or neutral/alkaline [3,5,9]. Mineralogic and chemical study of terrestrial analog sites rich in opaline silica may help inform ongoing rover investigations and help relate *in situ* rover studies to orbital observations through spectroscopy. Here we build on earlier work by [10] by comparing near-infrared reflectance spectra of silica-rich samples from volcanic fumarole (Hawaii) and hot spring (Yellowstone NP) environments to compare with differences in morphology, chemistry, and mineral assemblages associated with these environments.

**Methods:** Eighteen samples from Yellowstone and 47 samples from Hawaii were ground to <45  $\mu\text{m}$  powders and reflectance spectra were obtained from 0.4-2.5  $\mu\text{m}$  on an ASD spectroradiometer and 1.5-25  $\mu\text{m}$  on an FTIR spectrometer in RELAB at Brown University, all under ambient conditions. A spectral

continuum was fit and divided from each original spectrum to obtain the band depth of diagnostic Si-OH absorptions at  $\sim 2.21$ -2.35  $\mu\text{m}$ . Variations in these silanol absorptions are related to water content, which in turn may be related to maturity of the opal [10,11]. To quantify these spectral variations we also modeled these absorptions with Gaussians centered at 2.21 and 2.26  $\mu\text{m}$  and used the ratio of the 2.26/2.21 Gaussian amplitudes as a proxy for hydration state and possible opal crystallinity (e.g., opal-A versus -CT/C [10]).

XRD patterns of the same samples were obtained using a Bruker D2 Phaser (Cu source) in order to identify crystalline phases as well as the presence of an amorphous component observed at  $15^\circ$ - $35^\circ$   $2\theta$ . We use the area of this amorphous hump as a qualitative proxy for the amount of amorphous material in the sample. The area is calculated by subtracting a background-corrected pattern from the original XRD pattern from  $15^\circ$ - $35^\circ$   $2\theta$ , where the "background" is comprised of the amorphous hump (Fig. 1).

**Results:** Many samples from both Yellowstone and Hawaii appear to be rich in opal-A. The area of the XRD-amorphous hump correlates with the 2.21  $\mu\text{m}$  band depth for samples with significant XRD amorphous content and that also lack other minerals with 2.2  $\mu\text{m}$  absorption features (e.g., kaolinite) (Fig. 2). We therefore interpret the amorphous component as predominantly opal-A, consistent with spectral features (Fig. 1), though the additional presence of volcanic glass cannot be ruled out for all Hawaii samples.

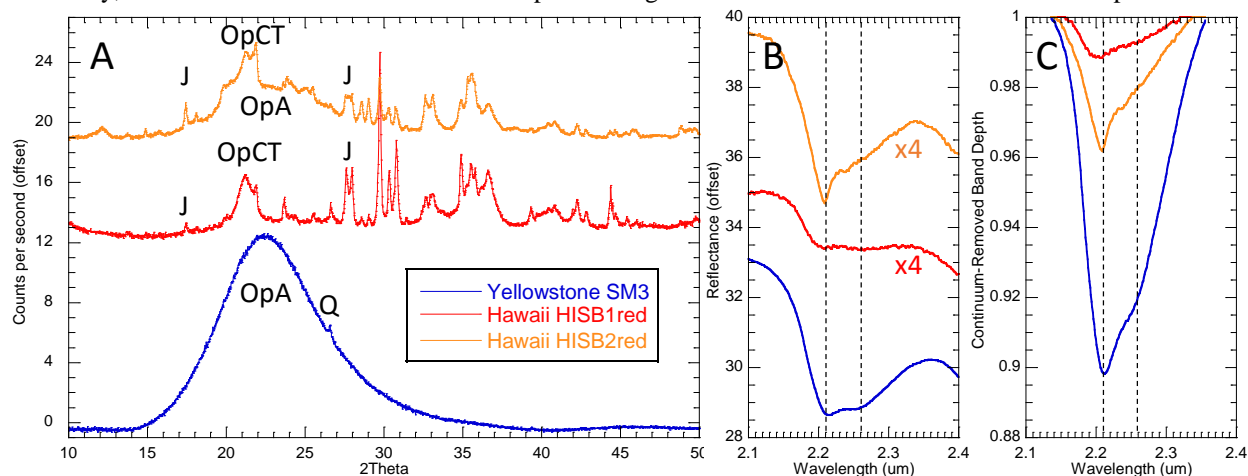
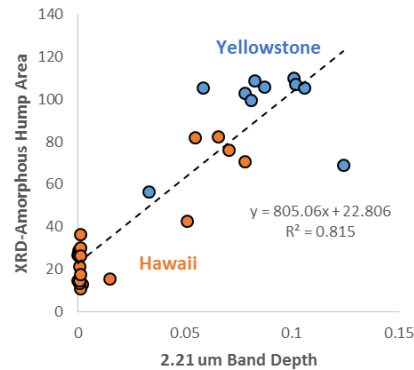


**Figure 1.** A) Select XRD powder patterns showing the variety of opaline silica in the sample suite, ranging from common opal-A (OpA) to more uncommon opal-CT (opCT). Note the relative purity of SM3 with quartz (Q) as the only crystalline phase, while the HISB samples contain jarosite (J) and other igneous minerals. Minerals that are not silica polymorphs or contributors to the 2.2  $\mu\text{m}$  feature are not labeled for clarity. B) Offset and scaled reflectance spectra of the same samples. C) Continuum-removed reflectance spectra to show relative band depths.

**Figure 2.**

Correlation of the 2.21  $\mu\text{m}$  band depth with the area of the XRD-amorphous hump for Yellowstone and Hawaii samples that contain opal-A as the sole 2.2  $\mu\text{m}$ -absorbing phase.



The Yellowstone samples also tend to have higher amorphous content relative to the Hawaii samples (Fig. 2), likely because they are primary precipitates instead of altered volcanic rocks. The Yellowstone samples are generally characterized by opal-A, discrete cristobalite, quartz, and tridymite. Kaolinite is present in the entire Rabbit Creek suite and one Nymph Lake sample. The majority of the other samples are taken from neutral/alkaline hot spring environments, with minor phases comprised of halite, orthoclase, and Ti-bearing phases such as anatase.

The mineralogy of the Hawaii suite is much more complex by comparison, with many igneous components (olivine, pyroxene, plagioclase) dominating the XRD patterns. Samples with opal-A tend to originate from Sulfur Banks, although smaller amorphous components are observed in the Mauna Ulu and Mauna Loa samples as well. Other silica polymorphs are discrete cristobalite, quartz, tridymite, and a few possible occurrences of opal-CT (Fig. 1). Other minerals in these samples that give rise to 2.2  $\mu\text{m}$  features are kaolinite, jarosite, gypsum and gibbsite. Ti-bearing minerals like anatase are also present.

While opal-A is a common aqueous alteration product at low temperatures, cristobalite and tridymite typically form at higher temperatures and could represent detrital materials in our samples, as is thought for tridymite found at Gale crater [4,5]. Surprisingly, very few of our samples exhibit XRD patterns consistent with opal-CT, suggesting either limited opal diagenesis or full conversion of some opal-A to cristobalite or quartz without preservation of the intermediate phases [12]. The prevalence of opal-A as opposed to opal-CT/C has also been suggested for martian deposits studied by rovers [4] and orbiters [13].

Despite both Yellowstone and Hawaii being dominated by opal-A (and not opal-CT/C), differences in the shape of the 2.2  $\mu\text{m}$  feature exist between the two sample suites. Yellowstone samples tend to have higher 2.26/2.21 band ratios (average=2.1) and greater variation in this ratio, indicating increased H-bonding in the opal, whereas Hawaii samples have a lower ratio (~1.7) and exhibit a narrower distribution (Fig. 3A).

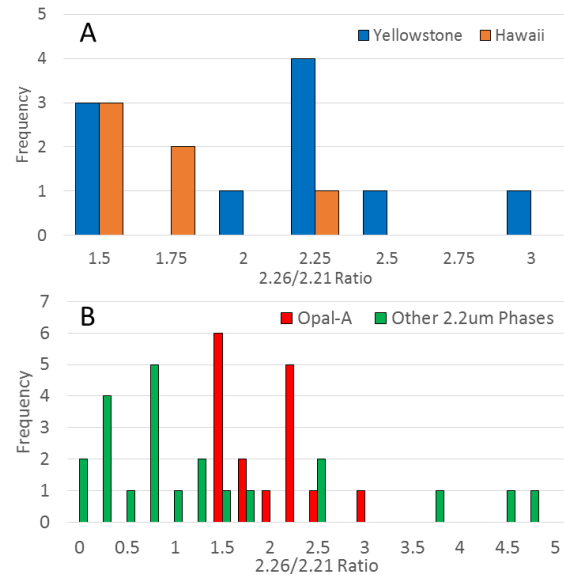


**Figure 3.** Histograms of the 2.26/2.21 ratio parameter for A) Yellowstone and Hawaii opal-A and B) samples rich in opal-A (red) and samples with 2.2  $\mu\text{m}$  features attributed to other phases such as kaolinite, jarosite, gypsum, and gibbsite (green).

Samples rich in opal-A seem to occupy a specific field in the 2.26/2.21 parameter space and range from ratios of 1.5 to 3. In contrast, samples bearing additional phases with 2.2  $\mu\text{m}$  features (e.g., kaolinite, jarosite) span the entire parameter space (with most ratios ranging from 0 to 5) and are concentrated at lower values (Fig. 3B).

**Conclusions:** Si-rich phases in samples from Yellowstone and Hawaii are dominated by opal-A, and spectral variations are observed between the two sample suites when using the 2.26/2.21 ratio parameter. Current results suggest variations in opaline silica spectra may reflect differences in degree of H-bonding, which may in turn be related to the different formation environments. Ongoing quantitative mineralogy and chemical measurements will help us to determine how chemical-mineral-spectral links may better inform us of silica-forming conditions on Mars at both rover and orbiter scales.

**References:** [1] Carter et al. (2013), *J. Geophys. Res.* 118, E004145; [2] Squyres et al. (2008), *Science* 320, 1063–1067; [3] Ruff et al. (2011), *J. Geophys. Res.* 116, E00F23; [4] Morris et al. (2016), *this conference*; [5] Frydenvang et al. (2016), *this conference*; [6] Bish et al. (2013), *Science* 341 (6153), 1238932; [7] Gellert et al. (2016), *this conference*; [8] Yen et al. (2016), *this conference*; [9] Hurowitz et al. (2016), *this conference*; [10] Rice et al. (2013), *Icarus* 223, 499–533; [11] Stolper (1982), *Contr. Min. and Pet.* 81, 1–17; [12] Tosca and Knoll (2009), *EPSL* 286, 379–386; [13] Milliken et al. (2008), *Geology* 36, 847–850.